19e Journées de l'Hydrodynamique
26 – 28 novembre 2024, Nantes

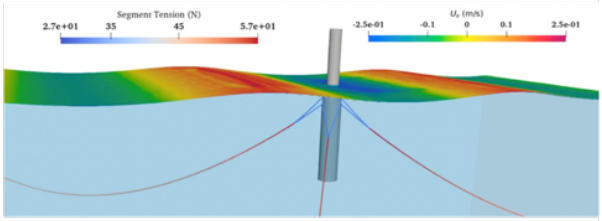

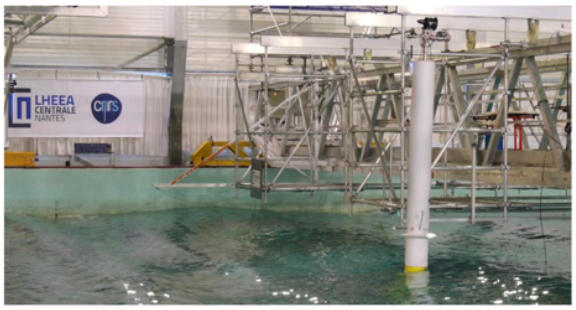

ELASTIC BAFFLE EFFECT ON LIQUID SLOSHING IN A FLEXIBLE TANK SUBJECTED TO COMPLEX EXCITATION

K.Q.N. KHA[1,2], M. BENAOUICHA[1,2], S.S. GUILLOU[2], A. SEGHIR[3]

kimquocnguyen.kha@segula.fr ; mustapha.benaouicha@segula.fr;
sylvain.guillou@unicaen.fr ; a.seghir@univ-bejaia.dz

[1]Segula Technologies, Naval and Energy Engineering Research and Innovation Unit, 9 avenue Edouard Belin, Rueil-Malmaison, 92500, France
[2]Université de Caen Normandie, LUSAC, EA 4253, Normandy University, 60 rue Max-Pol Fouchet, Cherbourg-Octeville, 50130, France
[3]Research Laboratory of Applied Hydraulics and Environment, Faculty of Technology, University of Bejaia, Targa Ouzemmour, Bejaia, 06000, Algeria

Résumé

Une chicane est une structure rigide ou souple placée à l'intérieur d'un réservoir de stockage partiellement rempli de liquide pour atténuer l'amplitude du ballottement et réduire les risques associées. Une chicane élastique immergée du liquide en ballottement dans un réservoir flexible soumis à une excitation externe complexe est ainsi considérée. Une méthodologie numérique a été développé pour prendre en compte l'interaction fluide-structure. Elle permet de coupler via la bibliothèque de couplage preCICE, deux codes opensource très efficaces : OpenFOAM pour le fluide et FEniCS pour le solide. La méthodologie numérique est d'abord validée avec des résultats expérimentaux issue de la litérature. Ensuite, une analyse du ballottement dans un réservoir soumis à une excitation sismique, en présence ou pas de chicane, rigide ou souple, est réalisée. L'étude comparative montre qu'une chicane élastique a un effet considérable sur l'amplitude du ballottement et l'oscillation des parois du réservoir. En outre, il a été montré que la flexibilité de la chicane joue un rôle déterminant sur l'atténuation de ces oscillations.

Summary

A baffle is a rigid or flexible structure, placed inside a storage tank partially filled with liquid to attenuate the amplitude of the sloshing and reduce the associated risks. An elastic baffle immersed in the sloshing liquid in a flexible tank subjected to a complex external excitation, is thus considered. A numerical methodology has been developed to take into account the fluid-structure interaction. It allows to couple via the preCICE coupling library, two very efficient open-source codes : OpenFOAM for the fluid and FEniCS for the solid. The numerical methodology is first validated with experimental results from the literature. Then, an analysis of the sloshing in a tank subjected to a seismic excitation, in the presence or not of a baffle, rigid or flexible, is carried out. The comparative study shows that an elastic baffle has a considerable effect on the amplitude of the sloshing and the oscillation of the tank walls. In addition, it has been shown that the flexibility of the baffle plays a determining role in the attenuation of these oscillations.

I – Introduction

Violent sloshing in a liquid storage tank, due to dynamic environments or during sudden changes in motion, can lead to instability, potential damage to the tank and even pose safety risks. Installing the baffles in tank offers an effective mitigating of sloshing, so-called anti-sloshing effect, which has been investigated by many numerical analysis. The effects on sloshing behavior of the baffle's height [1], the baffle's shape (vertical, horizontal, ring, T-shaped, etc...) [2, 3, 4], the number of baffles [5] and also the position of the baffle in the tank [6] have been studied. These works proved that the baffles play a key role in sloshing mitigation by reducing the liquid's movement and its associated forces within a tank.

Most sloshing studies have used the Volume of Fluid (VOF) method [7] or the Smoothed Particle Hydrodynamics (SPH) method [8] to capture the liquid free surface for simulating the two-phase fluid flow. The VOF method has proven to be a rigorous method to simulate a two-phase fluid system [9, 10, 11, 12]. The SPH method based on the Lagrangian approach, is also widely used with great success in modeling the two-phase flows.

The elastic baffles have been recently considered for sloshing mitigation to take advantage of its flexibility on the damping effect. It is then required to take into account the fluid-structure interaction (FSI) in numerical approach. In the study of Dinçer [13], the behavior of a highly elastic baffle in a water tank under earthquake excitation is considered experimentally and numerically. The numerical approach developed a coupled SPH-FEM (Finite Element Method) for FSI problem. The numerical results showed good agreements with the experimental data. Ren et al. [14] investigated numerically the sloshing flow interaction with an elastic baffle in a 2D rectangular tank under a harmonic excitation using a SPH framework. The results showed that the sloshing mitigation effect of an elastic baffle was better than that of a rigid baffle if the liquid filling level was lower than the baffle's height. Zhang et al. [15] proposed a δ^+-SPH method to simulate the sloshing flows with elastic structures. The method improved the stability and accuracy of the numeric results. A study of double elastic baffles was provided and showed that they were more effective than single baffle in attenuating sloshing heights and wall pressures. Although the effect of elastic baffle on sloshing has been considered in many recent researches, no study has taken into account the flexibility of the tank wall which can alter the behavior of sloshing and elastic baffle.

The present study investigates the effect of an elastic vertical baffle on the sloshing in a flexible tank subjected to seismic excitation, as well as on the deformations of the tank wall. The FSI problem is solved using the numerical methodology presented in [16], in which the fluid flow is solved using the Finite Volume Method (FVM) and the VOF approach for air-liquid interface tracking, implemented in the OpenFOAM code. The structure dynamics is solved using the Finite Element Method (FEM) in the FEniCS code and the fluid-structure interface is managed by the preCICE coupling library [17]. The paper is structured as follows. A description of studied geometry, the numerical methodology and its experimental validation are presented in Section II. The obtained results are discussed in Section III. Finally, a conclusion is drawn in Section IV.

II – Problem description and numerical methodology

II – 1 Elastic baffle submerged in a rectangular tank

A 2D partially water filled rectangular tank with the dimensions of $L_f = 30$ cm and $H_s = 25$ cm is considered. The tank is filled up to $H_f = 10$ cm and the tank thickness is $t_w = 1$ cm. The tank is considered flexible with the Young's modulus of 150 MPa. A vertical baffle having 3 mm thickness, 8 cm height and 10 MPa Young's modulus is fixed at the middle bottom of the tank. Figure 1 shows the tank geometry and the boundaries of computing domain. The tank is opened from top (atmospheric boundary Γ_{atm}), mounted at the bottom (Γ_w for the fluid domain, Γ_{ws}

for the tank wall domain and Γ_{wb} for the baffle domain) and bounded by the fluid-structure interfaces (Γ_{fsw} for the tank wall domain and Γ_{fsb} for the baffle domain).

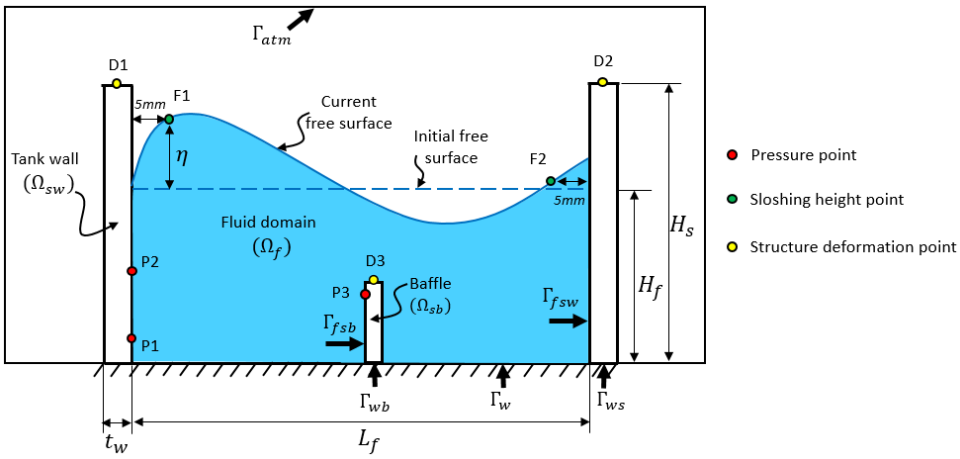

FIGURE 1 – 2D sketch of the vertical baffle in rectangular sloshing tank.

The free surface elevation (or sloshing height) defined as the distance between the air-water interface and the initial filled level, is extracted at the points (F1, F2) of 5 mm away from two sides of the tank walls. The deformations of the tank wall and the baffle are calculated at the top of the wall (D1, D2) and the baffle (D3). The pressure points are arranged on the tank wall (P1, P2) and the baffle (P3).

The tank is subjected to a horizontal seismic excitation. The seismic signal is taken as the 1952 Kern County earthquake (USA) recorded at the Pasadena - CIT Athenaeum ground station. The amplitude of Peak Ground Accelerations (PGA) is 0.1 g at 17.39 s. The time history and the Fast Fourier Transform (FFT) of the signal are depicted in Figure 2. The dominant frequencies are in the zone of $0-2$ Hz which is near the resonance. The highest FFT amplitude frequency is 0.78 Hz.

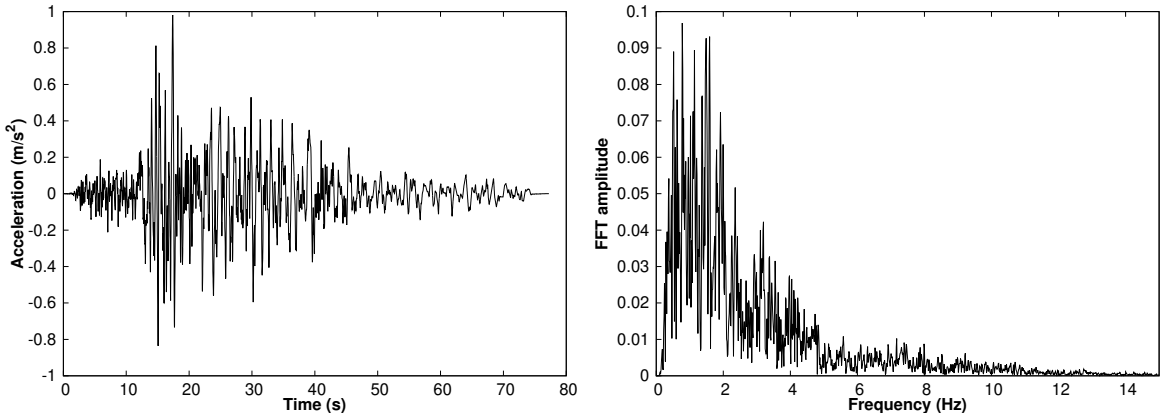

FIGURE 2 – Acceleration time history and acceleration spectrum of Pasadena seismic excitation..

II – 2 Numerical methodology

The unsteady and incompressible two-phase flow is governed by the Navier-Stokes equations (1) given in Arbitrary-Lagrangian-Eulerian (ALE) formulation.

$$\begin{cases} \nabla \cdot \mathbf{u} = 0 \\ \rho_f \dfrac{\partial \mathbf{u}}{\partial t} + \rho_f((\mathbf{u\text{-}w}) \cdot \nabla)\mathbf{u} = -\nabla P + \mu_f \nabla^2 \mathbf{u} + \rho_f(\mathbf{g} + \boldsymbol{A_e}) + \boldsymbol{f_\sigma} \\ \dfrac{\partial \mathbf{u}}{\partial \mathbf{n}} = 0 \quad \text{on} \quad \Gamma_{atm} \\ \mathbf{u} = 0 \quad \text{on} \quad \Gamma_w \\ \mathbf{u} = \dot{\boldsymbol{\xi}} \quad \text{on} \quad \Gamma_{fsw} \text{ or } \Gamma_{fsb} \\ \mathbf{u}(0) = 0 \quad \text{on} \quad \Omega_f \end{cases} \tag{1}$$

where ρ_f is the fluid mass density, $\mathbf{u}$ and $\dot{\boldsymbol{\xi}}$ are the fluid velocity vector and the local structure velocity vector, $\mathbf{w}$ is the grid velocity and A_e is the acceleration due to an external excitation. The fluid domain boundaries Γ_{atm}, Γ_w and Γ_{fs} are shown in figure 1(a). The normal unit vector $\mathbf{n}$ is pointing out the fluid domain. The VOF method [7] is adopted to track the interfaces between liquid and air phases.

The elastic deformations of the structure are governed by the following conservation equations (2). The boundary and initial conditions for the structure domain are also given.

$$\begin{cases} \rho_s \dfrac{\partial^2 \boldsymbol{\xi}}{\partial t^2} = \nabla \cdot \boldsymbol{\sigma_s} + \rho_s(\mathbf{g} + \boldsymbol{A_e}) & \\ \dot{\boldsymbol{\xi}} = \boldsymbol{\xi} = 0 & \text{on} \quad \Gamma_{sw} \text{ or } \Gamma_{sb} \\ \boldsymbol{\sigma_s} \cdot \mathbf{n} = \boldsymbol{\sigma_f} \cdot \mathbf{n} & \text{on} \quad \Gamma_{fsw} \text{ or } \Gamma_{fsb} \\ \dot{\boldsymbol{\xi}}(0) = \boldsymbol{\xi}(0) = 0 & \text{on} \quad \Omega_{sw} \text{ or } \Omega_{sb} \end{cases} \tag{2}$$

where ρ_s, $\boldsymbol{\xi}$ and σ_s are, respectively, the solid density, the local deformation of the structure and the Cauchy stress tensor. In this study, the considered structures are the tank wall and the baffle so the local deformation of the structure ξ corresponds to that of the tank wall ξ_w in the domain Ω_{sw} bounded by Γ_{sw}, Γ_{fsw} and that of the baffle ξ_b in the domain Ω_{sb} bounded by Γ_{sb}, Γ_{fsb}.

The fluid–structure coupled problem is solved using a strong implicit coupling scheme. At each time step, the fluid forces are transmitted from the fluid domain to the solid domain through the fluid–structure interface. Similarly, the solid deformations are transmitted to the fluid domain from the structure domain. These values at the fluid-structure interface are solved by the fixed-point equation. The procedure is detailed in [16].

II – 3 Validation of the numerical methodology

Dinçer [13] studied experimentally and numerically the deformations of the elastic baffle in a sloshing tank. The tank and the baffle dimensions were presented in figure 1. In the experiment, the tank was made of plexiglass with a 1 cm thickness so the tank walls can be assumed to be rigid. The tank was subjected to a horizontal one-cycle cosine excitation. Its acceleration can be written as $\mathbf{A_e} = a\omega_e^2 \cos(\omega_e t)$, with $a = 0.0135$ m and $\omega_e = 10.472$ rad/s. The external impulse was applied only during 0.6 seconds which represent one period of the signal.

Figure 3 shows the free surface profiles obtained from experiments, present simulations and numerical results of the reference at the instants when the maximum baffle deformations are obtained. It is observed that the sloshing and the baffle behaviors are consistent between reference and present numerical results. At $t = 0.69$ s, the free surface profile obtained from the present results is better than the reference numerical results, as it is closer to the experiments. Figure 4 shows that the horizontal deformations of the top baffle obtained from the present results are in good agreement with those from the experiments. These results demonstrate the efficiency of the present numerical methodology for studying the fluid-structure interaction problem.

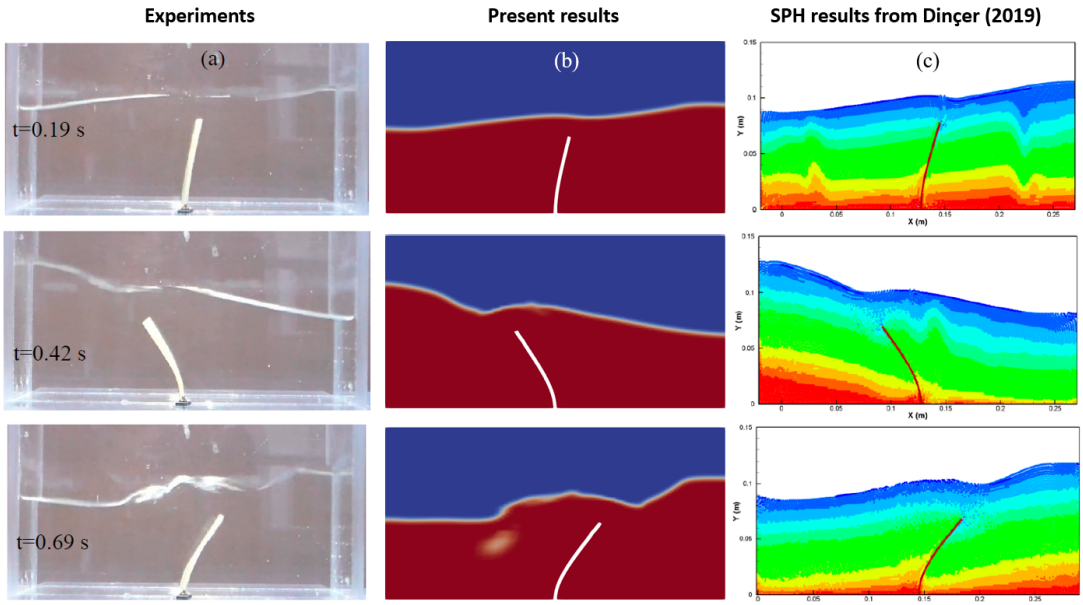

FIGURE 3 – Free surface profiles under one-cycle cosine impulse for (a) experiment given by Dinçer [13], (b) present simulation and (c) numerical results using SPH method from Dinçer [13].

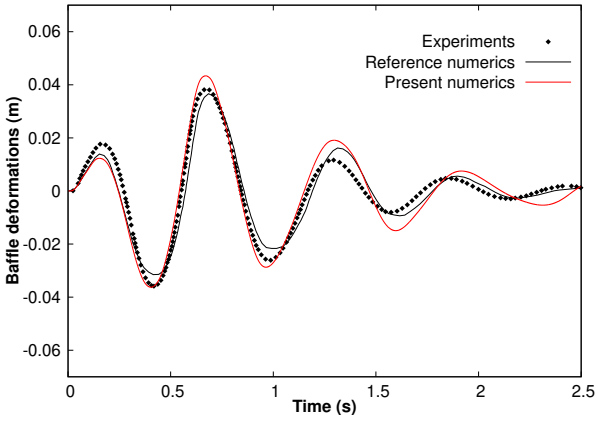

FIGURE 4 – Horizontal tip deformations of the elastic baffle under one-cycle cosine impulse obtained from present numerical results and from experimental and numerical results given by Dinçer [13].

III – Results

The first natural sloshing angular frequency in a rectangular tank without baffle can be determined by equation (3), taken from Faltinsen and Timokha [18] :

$$\omega_1 = \sqrt{\frac{\pi g}{L_f}\tanh\left(\frac{\pi H_f}{L_f}\right)} \tag{3}$$

The natural sloshing frequency calculated for the studied tank is $f_1 = \omega_1/2\pi = 1.43$ Hz. When the rigid baffle is added, the first natural sloshing angular frequency is changed to equation (4) :

$$\frac{\omega_1'^2}{\omega_1^2} = 1 - \frac{2\pi^2 \sin^2(\pi/2)}{\sinh(2\pi H_f/L_f)} \left(\frac{H_b}{L_f}\right)^2 \tag{4}$$

With H_b is the baffle's height. The natural sloshing frequency is then $f_1' = \omega_1'/2\pi = 1.15$ Hz.

The analytical structure eigenfrequency can be calculated from equation (5), according to Blevins [19] :

$$f_s = \frac{1.875^2}{2\pi H_s^2} \sqrt{\frac{EI}{\rho_s A_s}} \tag{5}$$

where I is the quadratic moment of the structure cross section and A_s is the area of the structure bottom. In this study, the analytical eigenfrequency of the tank wall and the elastic baffle is 6.46 Hz and 7.22 Hz, respectively.

To take into account the influence of the flexible tank, the Young's modulus of the tank wall is taken as 150 MPa. Three studied cases corresponding to a flexible tank without baffle, with rigid baffle and with elastic baffle are considered. The tank is under a seismic excitation presented in figure 2. Figure 5 presents the sloshing height obtained at two monitoring points F1 and F2. It can be seen in figure 5(a) and 5(b) that the presence of the baffle significantly reduces the free surface elevations. Indeed the maximum sloshing heights for the cases of elastic baffle and no baffle are, respectively, 0.117 m and 0.257 m at point F1 and 0.122 m and 0.375 m at point F2. A liquid spillage can be observed in the tank without baffle at $t = 25.3$ s and $t = 26.4$ s on the left and right tank walls, respectively. Furthermore, the elastic baffle also decreases the sloshing height compared to the rigid baffle case, especially after 20 seconds when the seismic excitation decreases significantly, see figure 5(c) and 5(d). Indeed, the maximum sloshing heights for the elastic baffle case are 0.117 m and 0.122 m, obtained at $t = 15.4$ s and $t = 15.7$ s at point F1 and point F2 respectively. Those for the rigid baffle case are 0.125 m and 0.122 m, obtained at $t = 30.5$ s and $t = 29.1$ s at point F1 and point F2 respectively.

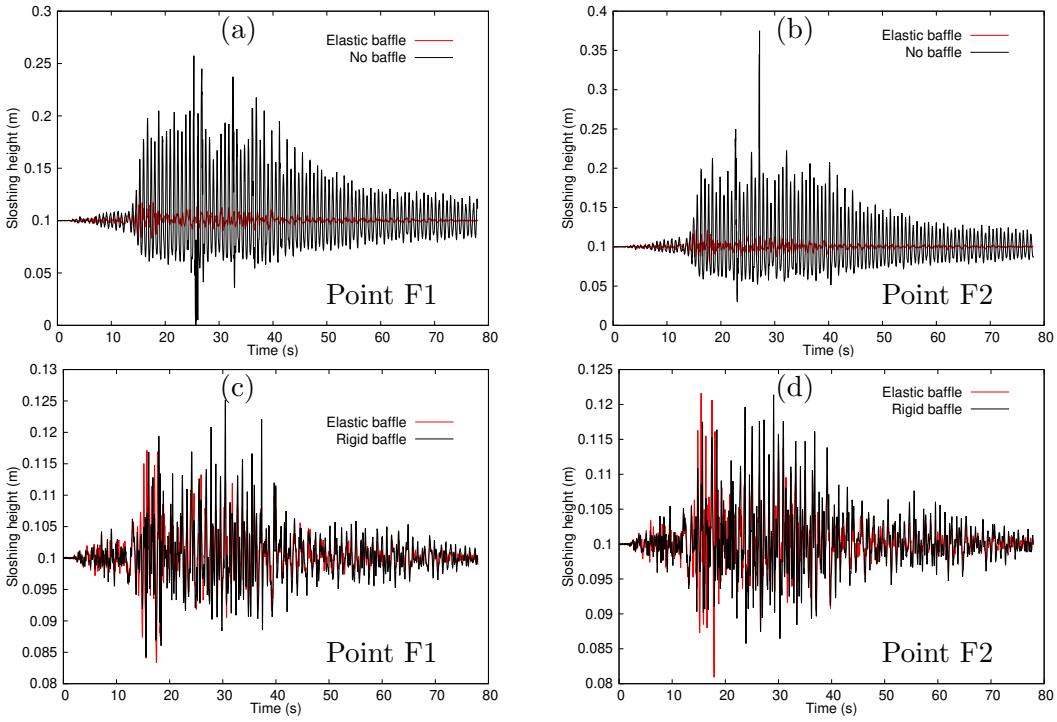

FIGURE 5 – Time evolution of the sloshing height for (a-b) the cases of elastic baffle and no baffle, and (c-d) the cases of elastic baffle and rigid baffle.

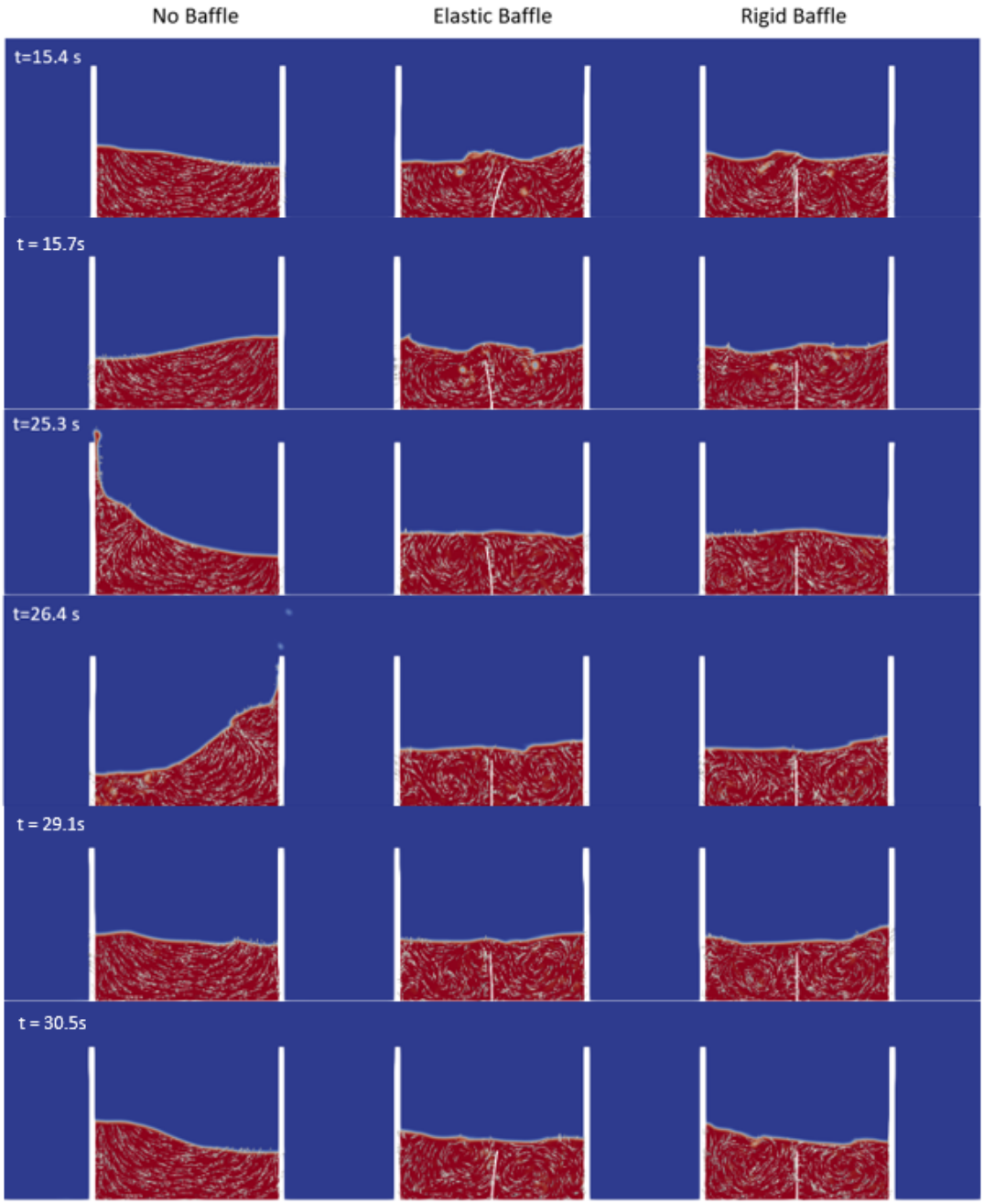

FIGURE 6 – Snapshots of the free surface profiles superposed by the liquid velocity vector for three studied cases.

Figure 6 presents the free surface profiles at the moments when the maximum sloshing heights are obtained for three studied cases. The sloshing mitigation is induced by the vortex between the baffle and the tank walls which leads to energy dissipation, as shown in figure 6. The dissipation reduces the amplitude and frequency of the sloshing waves, thereby minimizing the violent movement of the fluid. Indeed, as shown in figure 7, the FFT curve for the case without a baffle is much higher than that of the case with an elastic baffle and the natural sloshing frequency is reduced in case with a baffle. The natural sloshing frequency obtained for the ta baffle tank is 1.39 Hz, which represents a difference of 2.8 % compared with the analytical value of 1.43 Hz. For the tank with rigid baffle, the obtained value is 1.12 Hz, with a 2.6 % difference from the analytical one of 1.15 Hz. The same sloshing frequency is also obtained in the case of

a tank with an elastic baffle, although its FFT curve is different with that of rigid baffle. The natural frequency of the tank wall can also be seen in the FFT curve for the tank with baffle. This value is 6.77 Hz which represents a difference of 4.8 % from the analytical value of 6.46 Hz.

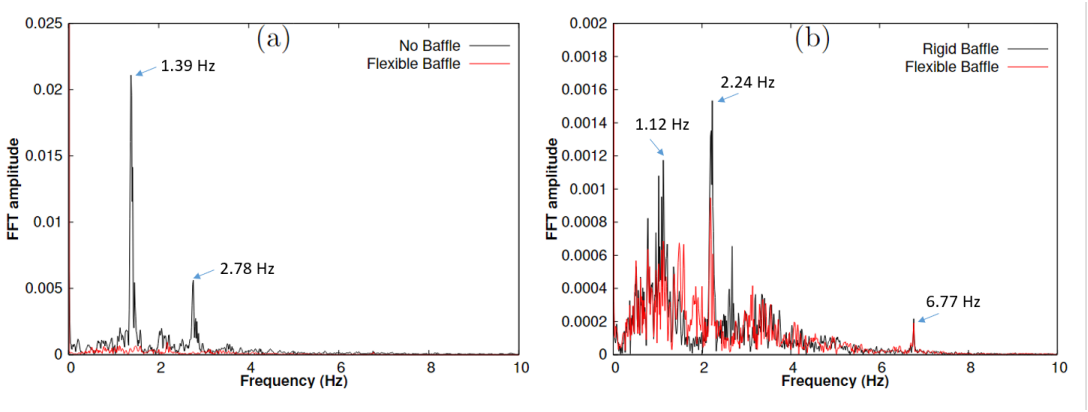

FIGURE 7 – FFT of the responses of sloshing height at point F1 for (a) the cases of elastic baffle and no baffle, and (b) the cases of elastic baffle and rigid baffle.

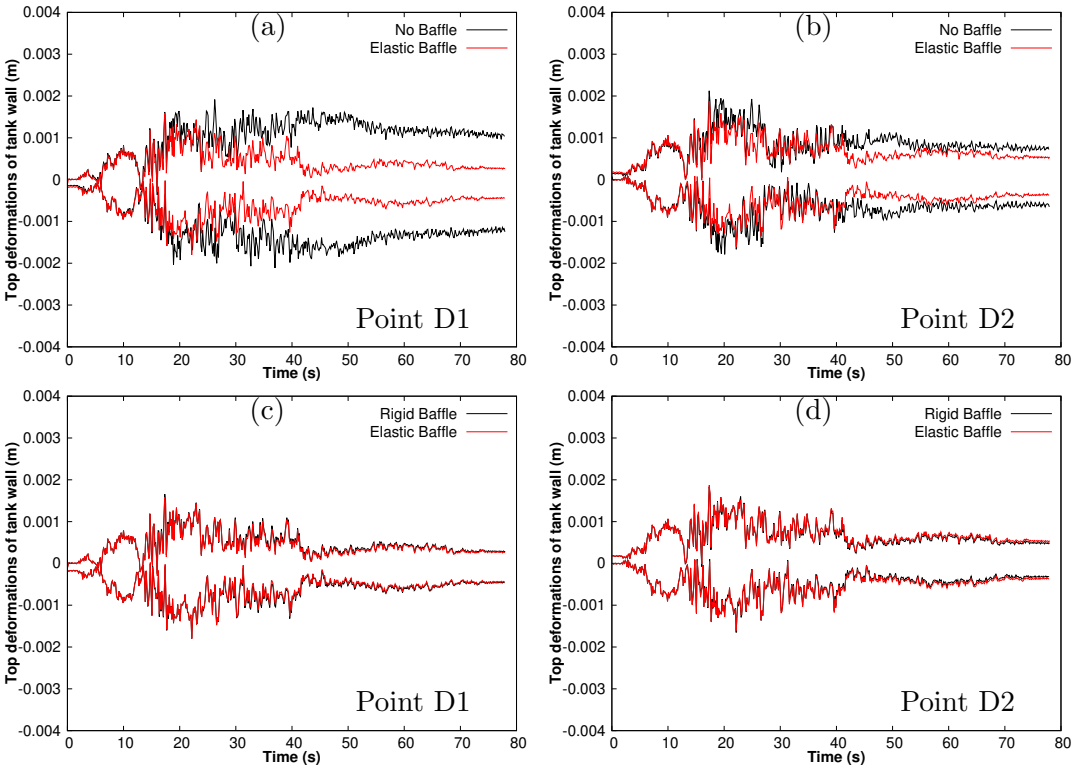

FIGURE 8 – Time evolution of the envelope of the left tank wall (point D1) and right tank wall (point D2) deformations for (a-b) the cases of elastic baffle and no baffle, and (c-d) the cases of elastic baffle and rigid baffle.

The evolutions of the envelope of the top tank walls deformations are presented in figure 8 for all studied cases. It can be seen that the baffle decreases the wall deformations on both left and right sides of the tank, as shown in figure 8(a) and 8(b). The maximum reduction of the tank wall deformations is about 75 % at point D1 and 50 % at point D2. It can be seen that the tank walls still oscillate even when the external forces become less significant after 40

seconds of seismic event. The deformation responses of the left and the right tank walls are also different. There is very slight difference between the influence of rigid and elastic baffles on the deformations of the tank walls, as displayed in figures 6(c) and 6(d). The relative difference between the two responses is about 5 %.

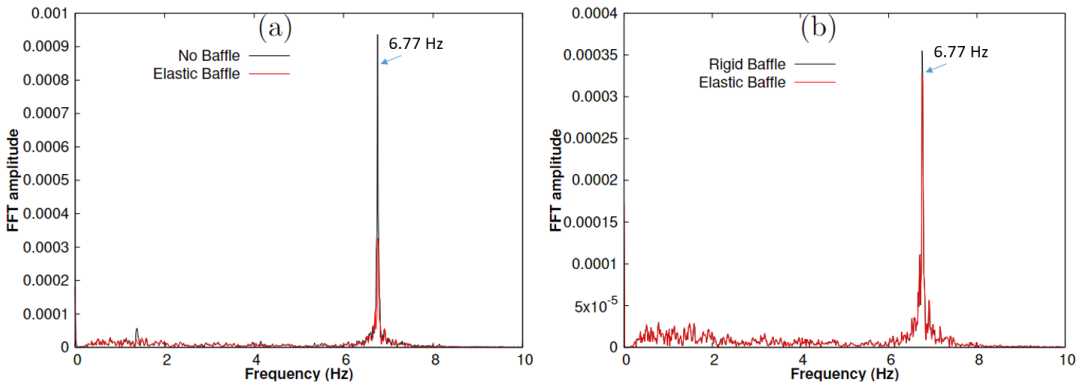

FIGURE 9 – FFT of the responses of tank wall deformations at point D1 for (a) the cases of elastic baffle and no baffle, and (b) the cases of elastic baffle and rigid baffle.

The FFTs of the wall deformations responses at point D1 are presented in figure 9. As observed in figure 9(a), the baffle case does not change the natural frequency of the tank wall. This calculated value is 6.77 Hz which is the same value obtained from the FFT of the sloshing height, see figure 7(b). The structural frequency is dominant compared to the excitation and sloshing frequencies. Since the difference of the wall deformations between the rigid and elastic baffle cases is very small, their corresponding FFTs are almost the same, see figure 9(b).

IV – Conclusions and perspectives

A numerical investigation of the elastic baffle behavior in a flexible sloshing tank subjected to horizontal seismic excitation has been presented. The two-phase flow problem coupled with the linear elastic solid problem was solved by coupling the OpenFOAM and FEniCS codes respectively, through the preCICE coupling library. The results demonstrated that the elastic baffle has a considerable effect on flow and tank walls oscillations. Specifically, the elastic baffle is more effective than the rigid baffle in attenuating the sloshing heights. It is worth noticing that the obtained results are valid for the studied seismic excitation, a parametric study is required to obtain a general conclusion. This issue will be considered in the future work.

Références

[1] J. Jung, H. Yoon, C. Lee, and S. Shin, "Effect of the vertical baffle height on the liquid sloshing in a three-dimensional rectangular tank," *Ocean Engineering*, vol. 44, pp. 79–89, 2012.

[2] R. Shamsoddini, "Numerical investigation of vertical and horizontal baffle effects on liquid sloshing in a rectangular tank using an improved incompressible smoothed particle hydrodynamics method," *Journal of Computational and Applied Research in Mechanical Engineering*, vol. 8, no. 2, pp. 177–187, 2019.

[3] U. Ünal, G. Bilici, and H. Akyıldız, "Liquid sloshing in a two-dimensional rectangular tank : A numerical investigation with a t-shaped baffle," *Ocean Engineering*, vol. 187, p. 106183, 2019.

[4] M. A. Xue and P. Lin, "Numerical study of ring baffle effects on reducing violent liquid sloshing," *Computers & Fluids*, vol. 52, pp. 116–129, 2011.

[5] C. Ma, C. Song, and G. Ma, "Numerical study on suppressing violent transient sloshing with single and double vertical baffles," *Ocean Engineering*, vol. 223, p. 108557, 2021.

[6] S. C. Jiang, A. Feng, and B. Yan, "Numerical simulations for internal baffle effect on suppressing sway-sloshing coupled motion response," *Ocean Engineering*, vol. 250, p. 110513, 2022.

[7] C. Hirt and B. Nichols, "Volume of fluid (vof) method for the dynamics of free boundaries," *Journal of Computational Physics*, vol. 39, pp. 201–225, 1981.

[8] J. Shao, H. Li, G. Liu, and M. Liu, "An improved sph method for modeling liquid sloshing dynamics," *Comput. Struct.*, vol. 100-101, pp. 18–26, 2012.

[9] D. Liu and P. Lin, "A numerical study of three dimensional liquid sloshing in tanks," *J. Comput. Phys.*, vol. 227 (8), pp. 3921–3939, 2008.

[10] S. Jiang, B. Teng, W. Bai, and Y. Gou, "Numerical simulation of coupling effect between ship motion and liquid sloshing under wave action," *Ocean Engineering*, vol. 108, pp. 140–154, 2015.

[11] H. Jin, R. Song, and Y. Liu, "Sloshing motion in a real-scale water storage tank under nonlinear ground motion," *Water*, vol. 12 (8), p. 2098, 2020.

[12] M. Xue, Z. Jiang, P. Lin, J. Zheng, X. Yuan, and L. Qian, "Sloshing dynamics in cylindrical tank with porous layer under harmonic and seismic excitations," *Ocean Engineering*, vol. 235, p. 109373., 2021.

[13] A. Dinçer, "Investigation of the sloshing behavior due to seismic excitations considering two-way coupling of the fluid and the structure," *Water*, vol. 11, no. 12, p. 2664, 2019.

[14] Y. Ren, A. Khayyer, P. Lin, and X. Hu, "Numerical modeling of sloshing flow interaction with an elastic baffle using sphinxsys," *Ocean Engineering*, vol. 267, p. 113110, 2023.

[15] G. Zhang, X. Yang, G. Liang, K. Zheng, and Z. Zhang, "Numerical simulation of sloshing flows with elastic structure by coupling δ^+-sph and spim," *Engineering Analysis with Boundary Elements*, vol. 165, p. 105764, 2024.

[16] K. Kha, M. Benaouicha, S. Guillou, and A. Seghir, "Numerical investigation of liquid sloshing in 2d flexible tanks subjected to complex external loading," *Journal of Fluids and Structures*, vol. 125, p. 104077, 2024.

[17] H. Bungartz, F. Lindner, B. Gatzhammer, M. Mehl, K. Scheufele, A. Shukaev, and B. Uekermann, "A fully parallel library for multi-physics surface coupling," *Computers Fluids*, vol. 141, p. 250–258, 2016.

[18] O. Faltinsen and A. Timokha, *Sloshing*. Cambridge University Press, 2009.

[19] A. Blevins, *Formulas for Natural Frequency and Mode Shape*. Krieger Publishing Company, 1979.